Research Article

Received: 7 June 2013 Revised: 2 October 2013 Accepted article published: 11 October 2013 Published online in Wiley Online Library: 11 November 2013

(wileyonlinelibrary.com) DOI 10.1002/pi.4634

# Relaxations and chain dynamics of sequential full interpenetrating polymer networks based on natural rubber and poly(methyl methacrylate)

Jacob John,[a,b*] Damir Klepac,[c] Mirna Petković Didović,[c] K. V. S. N. Raju,[d] Anitha Pius,[a] Mladen Andreis,[e] Srećko Valić[c,e*] and Sabu Thomas[f*]

## Abstract

**The relaxations of natural rubber (NR)/poly(methyl methacrylate) (PMMA) interpenetrating polymer networks (IPNs) were studied using dynamic mechanical analysis, electron spin resonance (ESR) and solid state NMR spectroscopy. Samples with a lower concentration of PMMA in IPNs (25 wt%) showed only one relaxation, which corresponds to NR with a slight shift to higher temperature. IPNs with 35 wt% of PMMA showed very broad transitions arising from $\beta$- and $\alpha$-relaxations in PMMA, with the $\beta$-relaxation slightly shifted to lower temperature. These compositions also showed a higher modulus at all temperatures. Highly phase separated IPNs showed a complete drop of modulus at 423 K. Higher crosslinking in the NR phase increases the miscibility and decreases the temperature difference between transitions, while in PMMA it increases the phase separation and does not affect the $\beta$-relaxation of the PMMA chains. The ESR results showed that PMMA chains located in the PMMA-rich and NR-rich domains have different motional characteristics. The strong interaction between PMMA and NR chains was also observed by carbonyl relaxation in solid state NMR spectra. It was found that medium level crosslinking is needed for better interpenetration between phases.**



**Keywords:** chain dynamics; electron spin resonance (ESR), spin probe; interpenetrating polymer networks; dynamic mechanical analysis

## INTRODUCTION

Interpenetrating polymer networks (IPNs) are a combination of two or more polymers in network form, in which at least one of the components is polymerized and/or crosslinked in the immediate presence of the other(s) (molecular interpenetration of networks).[1,2] In practice, most IPNs form immiscible compositions, usually phase separating during some stage of the synthesis. A sequential IPN is formed by swelling a polymer network of component A in the monomer of component B and then polymerizing. The physical laws that explain miscibility and phase separation in polymer blends are also applicable to IPNs. However, regarding phase separation some additional features have to be considered.[3–6]

Useful properties of polymer components in full IPNs are combined in order to overcome the drawbacks of individual components when they form blends. During this process, the molecular chain dynamics, which determine the properties of these polymers, change dramatically and this change depends on the level of mixing between the two components. The change is more pronounced when an elastic polymer is combined with a glassy one. The phase morphology in sequential IPNs is influenced by the miscibility of the polymer components, composition, crosslinking density, polymerization sequence (i.e. which polymer network is polymerized first as a pure network and which one is polymerized in the presence of the other component) and the kinetics of polymerization and phase separation.[7,8] Physical and mechanical properties of a particular IPN can be modified by varying (among other factors) the crosslinking density, and this is precisely the main reason for the growing interest in this kind of material.[9–15]

* *Correspondence to: Jacob John, Department of Chemistry, Gandhigram Rural University, Dindigul, Tamil Nadu 624302, India. E-mail: jacobparayil@gmail.com, Srećko Valić, Department of Chemistry and Biochemistry, School of Medicine, University of Rijeka, Braće Branchetta 20, 51000 Rijeka, Croatia. E-mail: svalic@medri.uniri.hr, Sabu Thomas, School of Chemical Sciences, Mahatma Gandhi University, P. D. Hills, Kerala 686560, India. E-mail: sabupolymar@yahoo.com*

a *Department of Chemistry, Gandhigram Rural University, Dindigul, Tamil Nadu 624302, India*

b *Department of Polymer Science and Engineering, 120 Governors Dr, University of Massachusetts-Amherst, Amherst, MA 01003, USA*

c *Department of Chemistry and Biochemistry, School of Medicine, University of Rijeka, Braće Branchetta 20, 51000 Rijeka, Croatia*

d *Division of Organic Coatings and Polymers, Indian Institute of Chemical Technology, Hyderabad 500607, India*

e *Rudjer Bošković Institute, Bijenička 54, 10000 Zagreb, Croatia*

f *School of Chemical Sciences, Mahatma Gandhi University, P. D. Hills, Kerala 686560, India*

Intermolecular constraints play an important role in the segmental dynamics of all polymer systems in the bulk state.[16] A particular case in this context is that of crosslinked polymers. Several studies have been reported on the influence of crosslinking degree on $\alpha$-relaxation analysed by different techniques, such as dielectric spectroscopy and dynamic mechanical analysis.[17–21] These studies revealed that the most striking effect caused by an increase in crosslinker concentration is the broadening of relaxation and the slowing down of segmental dynamics, which implies a shift of the transition region to longer relaxation times or lower frequencies. The cooperative character of $\alpha$- and $\beta$-relaxations in different temperature regions can be analysed by studying the influence of a second component in the form of an IPN on the mobility of polymer chain segments. Although there is some information about the secondary relaxation of poly(methyl methacrylate) (PMMA), the effect of blending on the local motions that originate from the secondary relaxation is not well understood. This relaxation process appears at lower temperatures and with lower apparent activation energy in miscible blends of PMMA with bisphenol-A polycarbonate.[22] It is also clearly shifted towards lower temperature in polyurethane and PMMA (PU/PMMA) IPNs with respect to pure PMMA.[23] Dynamic mechanical analysis (DMA) is one of the most powerful methods used in the investigation of heterogeneous polymeric systems, which enables the estimation of the elastic moduli, mechanical losses, glass transition temperatures, relaxation characteristics etc. and plays an important role both in a theoretical description of the systems and in their practical applications.

Electron spin resonance (ESR) spectroscopy (spin probe method) has been widely used to obtain information about motional behaviour and relaxation processes in polymers.[24–27] This technique generally uses paramagnetic species, commonly stable nitroxide radicals, which are dispersed (spin probes) or covalently attached (spin labels) to the polymer matrix. The ESR spectrum of a nitroxide radical depends on its rotational motion and is sensitive to the nitroxide mobility, with correlation times ($\tau_c$) in the range $10^{-7} - 10^{-11}$ s. Numerous studies have indicated that the mobility of the nitroxide radical is related to the dynamics of the host polymer.[28–31]

Spin probes reflect different environments in a given sample if the respective rates of motion are different.[30–32] If the nitroxide molecules are located in both phases of a heterogeneous two-component polymer system, the ESR spectra are composed of two components differing in their correlation times. A wide range of molecular motions can be studied, including those with very slow motion characteristics for polymers well below the glass transition temperature $T_g$ and those with fast motion characteristics (above $T_g$). The nitroxide rotational correlation times can be determined reliably from the experimentally observed ESR line shapes, which retain many of the features observed from a collection of randomly oriented immobilized or moving nitroxide molecules. Thus, the $\tau_c$ value provides relevant information about segmental dynamics and phase separation in IPN systems.[31,32]

Measurement of carbon spin–lattice relaxation in a rotating frame ($T_{1\rho}$) could give information on the local mobility of polymer chains and is therefore usually employed to investigate the effect of blending on the local motions in a polymer mixture. $^{13}C$ $T_{1\rho}$ relaxation times are sensitive to molecular motions with frequencies of *ca* 10–100 kHz. Spin diffusion between $^{13}C$ nuclei is slow compared with $^{1}H$ spin diffusion, especially under the condition of magic angle spinning. Therefore, $^{13}C$ $T_{1\rho}$ relaxation times are not partially averaged by spin diffusion as $^{1}H$ $T_{1\rho}$ relaxation times often are, and hence information on the motion of each specific site is retained.[33–35]

In our previous work the results of relaxation and chain dynamics in semi-IPNs based on natural rubber (NR) and PMMA were reported.[36] It was found that the rigid PMMA chains, which closely interpenetrated into the highly mobile NR network, impart motional restriction on nearby NR chains, and the highly mobile NR chains induce some degree of flexibility in the highly rigid PMMA chains. Moreover, molecular level interchain mixing was found to be more efficient at a PMMA concentration of 35 wt%, where the strong interphase contributed to the large fraction of slow component in ESR spectra at higher temperatures. The ESR results were correlated to the morphology of semi-IPNs, as observed by SEM. $^{13}C$ $T_{1\rho}$ measurements of PMMA carbons indicated that the molecular level interactions were strong irrespective of the immiscible nature of the polymers.

Morphology, mechanical properties, thermal stability and gas transport behaviour of full IPNs based on NR and PMMA have been investigated using various techniques.[37] The crosslinking level of the two phases facilitates deeper interpenetration between the networks and has noticeable effects on the compatibility of immiscible components during IPN formation.

The present study aims to investigate the phenomenon of phase mixing in full IPNs, the effect of crosslinking on molecular mixing, the relaxation behaviour of the two components, and the motional characteristics of the polymer chains as a function of temperature, composition, crosslink density and intermolecular interaction that affect molecular motion using DMA, ESR (spin probe method) and the solid state NMR relaxation technique.

## EXPERIMENTAL

### Materials

High molecular weight NR ($M_w \approx 500\,000 - 900\,000$) was supplied by Rubber Research Institute of India, Kottayam, Kerala. Dicumyl peroxide (99%), the crosslinker for NR, was purchased from Aldrich and used as received. Methyl methacrylate (MMA, Aldrich) and ethylene glycol dimethylacrylate (EGDMA, Aldrich), the crosslinker for MMA, were distilled under vacuum prior to use. Azobisisobutyronitrile (AIBN, Aldrich), the initiator for MMA polymerization, was purified by recrystallization from methanol.

### Preparation of IPNs

Sheets of crosslinked NR (1–2 mm thick) were weighed and kept immersed in a homogeneous mixture of MMA, EGDMA and AIBN (0.7 g per 100 g of MMA). The NR sheets were swollen for various time intervals to obtain different weight percentages of PMMA. The swollen samples were kept for a few hours at 273 K to achieve an equilibrium distribution of the MMA monomer in the matrix. These swollen networks were heated at 353 K for 6 h and at 373 K for 2 h in an atmosphere of MMA to complete the polymerization and crosslinking of MMA. Four IPN samples were made with the following ratios of NR and PMMA: 75:25 ($NIM_{25}$), 65:35 ($NIM_{35}$), 50:50 ($NIM_{50}$) and 40:60 ($NIM_{60}$). Concentrations of crosslinker in weight percentage per 100 g for the NR and PMMA phases are denoted as superscripts before ($^{x}$) and after ($^{y}$) the sample's symbol, respectively. Thus, a general symbol for all the IPN samples is $^{x}NIM^{y}_{z}$ where *x* stands for wt% of crosslinker for the NR phase, *y* stands for wt% of crosslinker for the PMMA phase and *z* stands for wt% of the PMMA phase in the IPN sample. The obtained IPNs were kept in vacuum to eliminate residual unreacted MMA. The composition of the IPN samples was determined on



  

the basis of their final weights. The solitary EGDMA-crosslinked PMMA network was polymerized using the same procedure as for the IPNs.

### Dynamic mechanical analysis

DMA studies were performed on a Rheometrics DMA IV. Measurements were conducted in tensile mode at a frequency of 1 Hz in the temperature range 188–473 K. The heating rate was 3 K $min^{-1}$, and the results shown in this work are the mean value of three measurements (the errors were less than 5%).

### ESR measurements

The free nitroxide radical 4-hydroxy-2,2,6,6-tetramethylpiperidine-1-oxyl (TEMPOL) was used as a spin probe for ESR measurements. TEMPOL was chosen to study the investigated semi-IPNs since this spin probe was successfully used earlier for the study of natural rubber and similar systems.[32] The probe molecules were incorporated into IPN samples by swelling the samples in the probe solution. The mass of each sample was 40 mg. The temperature was kept constant (308 K) during 3 days of the probe incorporation process. Throughout this period, the probe molecules diffused into swollen IPN networks. At the same time, the solvent was slowly removed from the solution by evaporation. However, a small amount of solvent is usually trapped in the higher density regions of the samples. For this reason the samples were annealed in vacuum at 333 K and weighed from time to time. When their masses remained unchanged as a function of annealing time, the residual solvent was completely removed. The total amount of probe molecules in the samples was 0.15 wt%.

ESR measurements were performed on a Varian E-109 spectrometer operating at 9.2 GHz, equipped with a Bruker ER 041 XG microwave bridge and a Bruker ER 4111 VT temperature unit. Spectroscopic parameters were microwave power 2.0 mW, modulation amplitude 0.1 mT, scan range 10 mT and scan time 60 s. Spectra were recorded in a wide temperature range from 183 K to 413 K in steps from 5 K to 10 K, depending on the sensitivity of spectral line changes within each temperature region. The rigid limit spectra were recorded at 100 K for all samples. Samples were kept at the temperature of measurement for at least 10 min before the accumulation started. EW (EPRWare) Scientific Software Service program was used for data accumulation and manipulation. The number of accumulations varied from two to five depending on the signal to noise ratio.

### $^{13}C$ $T_{1\rho}$ relaxation measurements

Solid state $^{13}C$ cross-polarization magic angle spinning NMR spectra were recorded on a Bruker 300 MHz spectrometer, operating at 75.46 MHz frequency for $^{13}C$ nuclei. Samples were spun at a spinning speed of 3.1 kHz. The 90° pulse time was 4.5 µs, corresponding to a spin-locking field strength of 40 kHz. $^{13}C$ $T_{1\rho}$ measurements were performed by applying a $^{13}C$ spin-locking pulse after a 2 ms cross-polarization (CP) step. The decay of the $^{13}C$ magnetization in the spin-locking field was followed for spin-locking times of up to 14 ms.

## RESULTS AND DISCUSSION

### DMA — storage modulus and relaxations of IPNs

DMA scans of NR, PMMA and IPNs of different compositions are shown in Fig. 1. A decrease in modulus around 203 K, as usually observed, arises from a relaxation process in NR, while a sudden drop in the modulus of PMMA is due to its glass transition.

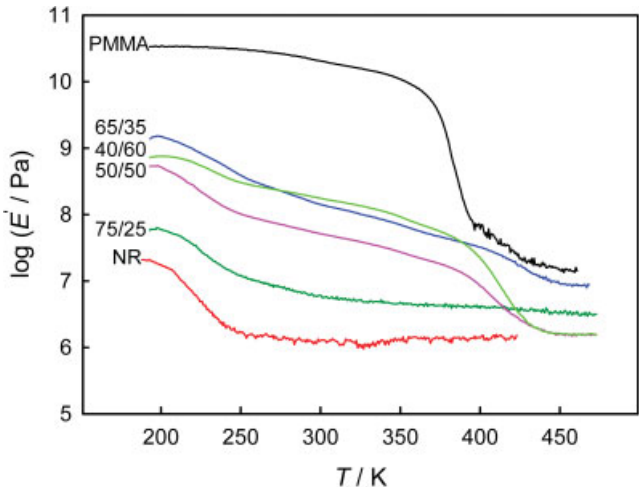


**Figure 1.** Storage modulus of PMMA ( – ), $^{0.8}NIM^{4}_{25}$ ( – ), $^{0.8}NIM^{4}_{35}$ ( – ), $^{0.8}NIM^{4}_{50}$ ( – ), $^{0.8}NIM^{4}_{60}$ ( – ) and NR ( – ) as a function of temperature.

The dynamic mechanical behaviour of full IPNs, especially with a lower concentration of PMMA, shows some very interesting behaviour compared with semi-IPNs of the same composition.[36] A considerable increase in the storage modulus values was observed in $^{0.8}NIM^{4}_{25}$ with a higher magnitude of increase compared with the analogous semi-IPNs.[36] Even though a high temperature transition is not present, the influence of PMMA can be seen in the inward shift of the transition and the decreased slope along with an increase in overall storage modulus. Here the crosslinking of the second component enhanced the interpenetration of rigid PMMA chains more effectively into the entangled NR network, indicating that some degree of enforced miscibility was obtained *via* IPN synthesis.[37] The SEM analysis showed that the system possesses a sea-island morphology with very small PMMA domains scattered all over the NR matrix.[37] The inward shift in transition is also a proof of some degree of molecular level mixing achieved during IPN formation.

A dramatic increase in the storage modulus with a completely different dynamic mechanical behaviour is observed for the sample $^{0.8}NIM^{4}_{35}$, which has a higher PMMA concentration compared with other NR/PMMA compositions of the same series. At low temperature, this composition shows the highest storage modulus comparable with that of $^{0.8}NIM^{4}_{60}$ at high temperature. The absence of a sharp transition with respect to NR and PMMA reveals the degree of mutual influence due to phase mixing obtained during IPN formation. This particular composition shows the highest phase mixing among all studied samples.

The increase in modulus values and the shape of the curve show that PMMA domains dispersed in NR phase act as a reinforcing agent because the modulus of the dispersed particles is higher than that of the matrix. However, the effect of a possible contribution of interpenetrated PMMA chains into the NR network which also induces motional restrictions on the highly mobile NR network cannot be excluded.[36]

At 50:50 composition ($^{0.8}NIM^{4}_{50}$), the two transitions corresponding to each component can be seen and the magnitude of the drop indicates that both phases became continuous. This suggests the formation of a double-phase network where each phase preserves the original molecular structure. Thus, the existence of two mechanical relaxations is clearly proved by the temperature behaviour of the storage modulus $E'$ in the above



  

composition and two well defined drops are observed in the regions of temperature where tan $\delta$ shows the main $\alpha$-relaxation peaks. The two transitions in $^{0.8}NIM^{4}_{60}$ can be seen with a sharp drop in the storage modulus at the glass transition region of PMMA. The magnitude of the drop suggests that the PMMA network is more continuous than the NR network at this composition. This composition shows the highest value of storage modulus in the intermediate region between the two transitions with modulus values comparable to those of $^{0.8}NIM^{4}_{35}$. Co-continuous morphology observed at this particular composition contributes to this observation.

An interesting observation in samples $^{0.8}NIM^{4}_{35}$ and $^{0.8}NIM^{4}_{25}$ is that these IPNs retain storage modulus values up to 473 K and these values are higher compared with pure NR and with IPNs with higher concentration of PMMA ($^{0.8}NIM^{4}_{50}$ and $^{0.8}NIM^{4}_{60}$). This is due to the effect of chain mixing at the molecular level and the development of an interlocking structure between the two components. In this case, the first formed phase (NR) is in the form of a three-dimensional network. During the simultaneous process of polymerization and crosslinking of the MMA component, the PMMA network has to grow interpenetrating in random directions through the available space in the NR network. The interpenetration of PMMA networks through NR networks due to simultaneous polymerization and crosslinking leads to a close mixing between the two components, which results in an enforced miscibility.[37] The random orientation along with the higher crosslinking (4 wt% EGDMA compared with 0.8 wt% dicumyl peroxide) locks the rigid PMMA network inside the three-dimensional NR network. The development of the above mentioned two situations in the structure leads these IPNs to follow the modulus of PMMA at higher temperature, as seen in Fig. 1. Here, the NR network chains are forced to follow the motions of the rigid PMMA network and so the entire matrix reflects a considerable degree of PMMA behaviour. The higher crosslinking degree of the PMMA network also contributes to the observed phenomenon. Both other compositions show the characteristics of a highly phase separated system and the modulus drops sharply at the softening point of PMMA to the value of a pure NR network, indicating no contribution from the crosslinked PMMA networks at higher temperature compared with the other two IPNs. This phenomenon observed at higher temperature is strong proof of a considerable degree of phase mixing during IPN synthesis with PMMA in the concentration range from 20 wt% to 40 wt%.

DMA results are useful to understand the behaviour of the main relaxation in the IPNs because the $\alpha$-relaxation predominates over local $\beta$-relaxation in DMA.[21] Figure 2 shows the relaxations of NR, PMMA and IPNs with varying PMMA concentrations. In the case of NR, the maximum of tan $\delta$ is observed around 203 K ($T_g$ of NR) while PMMA clearly shows the $\beta$- and $\alpha$-relaxations. The secondary relaxation appears as a broad peak with a maximum at 308 K. Both crosslinking and the IPN composition hardly shift the $\beta_{max}$ position, while the maximum of tan $\delta$ corresponding to the $\alpha$-relaxation is shifted to higher temperature mostly due to crosslinking. These changes in the dynamic mechanical data have already been observed for PMMA samples crosslinked with EGDMA.[38] The increase of the apparent $T_g$ of PMMA can be explained by an increase in the chain connectivity that leads to a decrease of the free volume and hence to the slowing down of relaxation dynamics as the crosslinker concentration increases.[9]

The influence of lower PMMA concentrations can be seen in the relaxations of the IPNs. As seen from the storage modulus sweep, the $^{0.8}NIM^{4}_{25}$ sample exhibits only one main relaxation

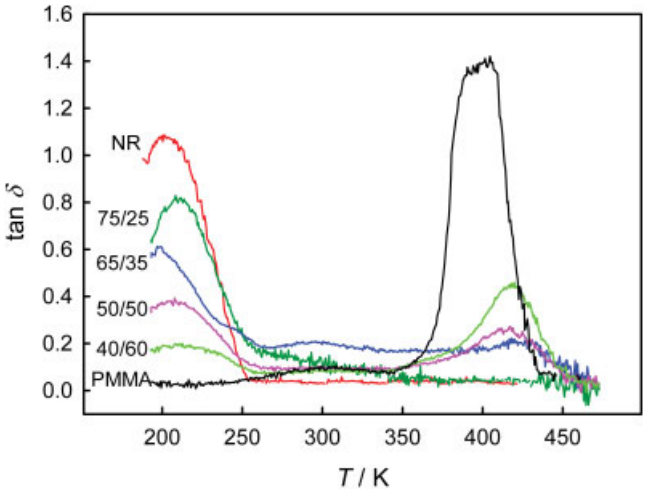


**Figure 2.** tan $\delta$ of PMMA ( – ), $^{0.8}NIM^{4}_{25}$ ( – ), $^{0.8}NIM^{4}_{35}$ ( – ), $^{0.8}NIM^{4}_{50}$ ( – ), $^{0.8}NIM^{4}_{60}$ ( – ) and NR ( – ) as a function of temperature.

corresponding to NR. The influence of PMMA can be noticed in the inward shift of the $\alpha$-relaxation of the NR component with a broad peak compared with that of pure NR. This is an indication of mixing at the molecular level which results in the overlapping of several relaxation processes, corresponding to regions rich in neat NR with others rich in neat PMMA. This reveals that most of the rigid PMMA network chains are in close proximity to the highly mobile NR network to influence the $\alpha$-relaxations of the NR phase. PMMA chains impart restrictions on the motional behaviour of the nearby NR chains and vice versa shifting the $\alpha$-relaxation of NR to higher temperature. In addition, the shift to higher temperature by about 20 K of the $\alpha$-relaxation peak of PMMA in the IPNs, compared with that of the solitary PMMA network, reflects the restrictions on macromolecular mobility imposed by the IPN intertwined network structure.

Sample $^{0.8}NIM^{4}_{35}$ has a different relaxational behaviour among all the IPNs we analysed. Apart from a complete peak shift observed in the $^{0.8}NIM^{4}_{25}$ sample, this composition does not show any shift in the $\alpha$-relaxation peak of the NR component (Fig. 3). The majority of the NR chains are undergoing $\alpha$-relaxation around 203 K. However, those highly mixed with the PMMA chains become more rigid and reflect the motional behaviour of chains with higher $T_g$. These NR chains are moving at a lower frequency compared with those far from PMMA. Thus, the relaxation times of NR chains are different from those which are very close and far away from the rigid PMMA networks. This results in a distribution of relaxation times and leads to broadening of the transitions.

Both phases seem to have more interaction between each other with very strong $\beta$-relaxations of PMMA at this particular composition. Relaxation of this sample in comparison with the homopolymers is shown in Fig. 3. It is very interesting that the peak showing the secondary relaxation of PMMA in $^{0.8}NIM^{4}_{35}$ is slightly shifted to lower temperature with respect to solitary PMMA. We shall provide a molecular explanation for this behaviour which was already reported in the case of PU/PMMA IPNs.[23]

The $\beta$-relaxation of PMMA arises out of the hindered rotation of the $-COOCH_3$ group around the C–C bond linked to the main chain. It has been found that the position of this relaxation depends only on the size of the lateral group and it is independent of the crosslinking degree due to the nature of the motions involved (localized motions).[9] In the above case, the deeper



  

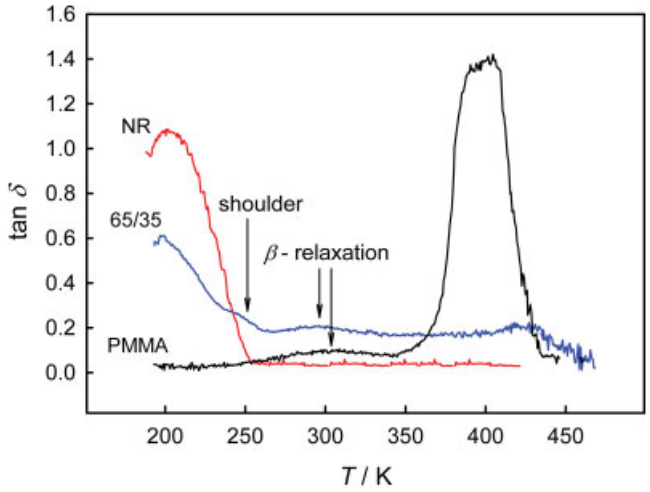


**Figure 3.** Shift of the $\beta$-relaxation of PMMA in $^{0.8}NIM^{4}_{35}$ ( – ) compared with solitary PMMA ( – ).

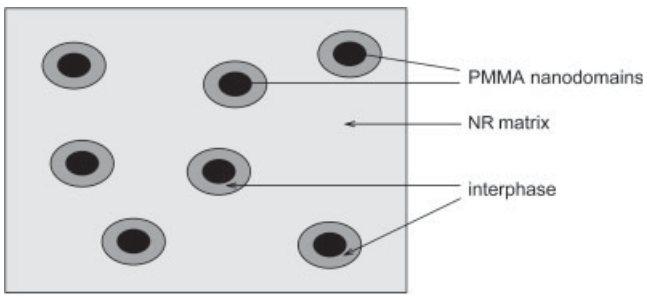


**Figure 4.** Schematic presentation of the morphology of nanostructured $^{0.8}NIM^{4}_{35}$ IPN showing the development of a strong interphase between the nanodomains of PMMA and the NR matrix.

interpenetration of the PMMA network in the continuous NR network reduces the stiffness of the PMMA chains. Thus, the PMMA chains become more flexible and exhibit more motional freedom in the highly mobile NR matrix. This higher mobility and motional freedom reduces the hindrance to the rotation of the $-COOCH_3$ group and the ester group is able to move at lower temperature resulting in a slight shift of the $\beta$-relaxation to lower temperature compared with solitary PMMA. Therefore the PMMA chains intimately mixed with the NR networks reach $T_g$ at a lower temperature than those embedded in the PMMA-rich region. This chain mixing leads to a broad distribution of $T_g$ over a temperature range of more than 60 K, as observed by DSC measurements.[37] Also, the tan $\delta$ of this particular composition shows maximum height in the intermediate region between the two main relaxations, which is a direct measure of miscibility.

However, a strong shoulder at the high temperature side of the NR relaxation (around 250 K) clearly describes the motional heterogeneity of the NR network. Two motionally distinct regions found in NR are due to the presence of sol and gel phases.[39] Motional restrictions in the gel phase are additionally supported by a deep penetration of PMMA networks in the NR matrix. Sample $^{0.8}NIM^{4}_{35}$ is found to form a strong interphase resulting in four distinct relaxations in the tan $\delta$ sweep. The morphology of this IPN is shown schematically in Fig. 4.

The IPNs with a higher concentration of PMMA (50 wt% and 60 wt%) show two broad peaks corresponding to the two main relaxations, characteristic of a phase separated system (Fig. 2). The intensities of the peaks are the same in the case of the 50:50 composition which is a measure of the continuity of the phases. At 60 wt%, the PMMA network becomes the major phase.

The influence of crosslinking of both phases is studied by varying the crosslink density of one phase while that of the other phase is kept constant. For this purpose, IPNs with three different levels of crosslinking and the same composition (50:50) were prepared. Figure 5(a) shows a comparison of the storage modulus of these samples. The loosely crosslinked IPN exhibits two sharp decreases in modulus values, corresponding to the $T_g$ values of the two phases. Due to the low NR crosslinking, the PMMA phase is more continuous compared with the other two IPNs. This continuity contributes to the higher storage modulus observed below the $T_g$ of PMMA and a sudden drop in $E'$ value above $T_g$. Higher crosslinking of NR makes the NR phase more continuous during IPN formation and results in lower storage modulus values below the $T_g$ of PMMA. The highly crosslinked IPN shows a sharp drop in $E'$ after the NR transition. At the softening point of PMMA (423 K), this sample shows a higher storage modulus compared with the other two. This behaviour can be understood as a consequence of some degree of phase mixing related to the loss tangent peaks (Fig. 5(b)). The higher crosslinking in the NR phase results in an inward shift of $T_g$ values of both phases – an indication of enhanced phase mixing. Medium crosslinked IPN shows a shift of about 15 K to lower temperature for the PMMA transition, while the highly crosslinked sample shows a maximum inward shift in the lower transition region. It is obvious that higher crosslinking leads to broadening of the transition due to overlapping of several relaxation processes.

The effect of crosslinking in the PMMA phase was also investigated. Figure 6(a) shows that loosely crosslinked PMMA has a maximum storage modulus at all temperatures because lower crosslinking in PMMA favours more continuity in the PMMA phase. Loss tangent peaks of these IPNs (Fig. 6(b)) reveal that a higher crosslinker amount (6%) in the PMMA phase increases the phase separation resulting in slight outward shifts of the two transitions of NR and PMMA. It also seems that higher crosslinking in the PMMA has no effect on $\beta$-relaxation. A medium crosslinker amount (4%) is preferable to maintain some degree of phase mixing. This can be deduced from the slight shift of the peak to lower temperature.

### ESR spin probe analysis

The ESR spectra of spin probes in IPNs with different compositions and crosslink densities were measured in the temperature range 193–413 K at intervals of 10 K or less. Figure 7 shows selected ESR spectra of spin probed pure NR, IPNs with different compositions ($^{2}NIM^{2}_{25}$, $^{0.8}NIM^{4}_{35}$, $^{2}NIM^{2}_{50}$, $^{4}NIM^{6}_{50}$, $^{4}NIM^{8}_{50}$, $^{0.8}NIM^{4}_{60}$) and solitary PMMA. The spectra of IPNs in the low temperature region are similar to those of pure NR and solitary PMMA. The central line in the spectra of IPNs at higher temperature has higher amplitude compared with the spectrum of pure NR, suggesting anisotropic rotational dynamics. In the temperature range 293–390 K, spectra consist of two components differing in their outer extrema separation and line shapes. These two spectral components correspond to the spin probes embedded in different motional environments, indicating the existence of microphase separation. At higher temperatures, the spectrum of pure NR shows two well resolved components, the slow and fast components being attributed to probe molecules embedded in the gel and sol phase, respectively.[39] The spectrum of solitary PMMA consists of two less resolved components due to the very



  

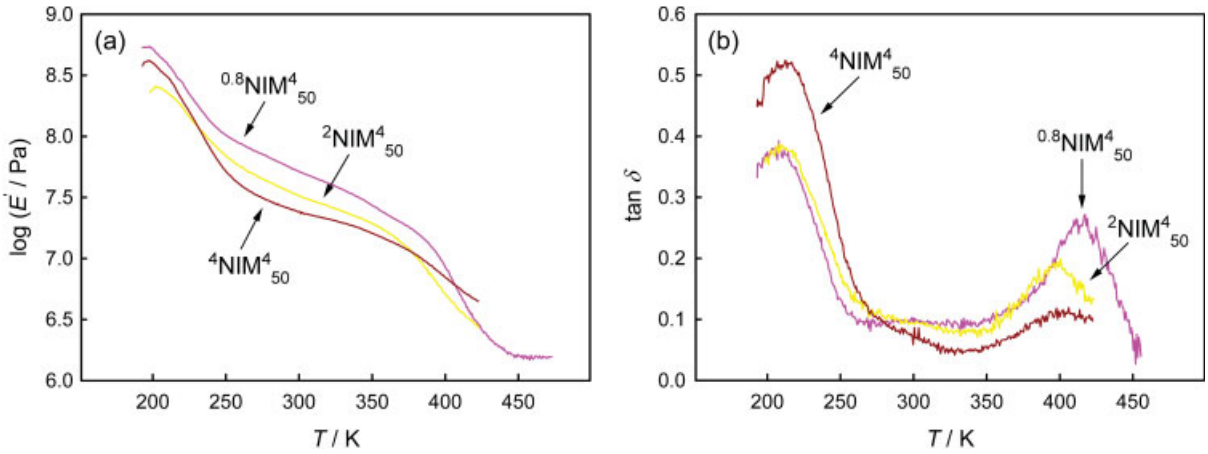


**Figure 5.** Effect of the crosslinking level of NR on the storage modulus (a) and relaxations (b) of $^{0.8}NIM^{4}_{50}$ ( – ), $^{2}NIM^{4}_{50}$ ( – ) and $^{4}NIM^{4}_{50}$ ( – ).

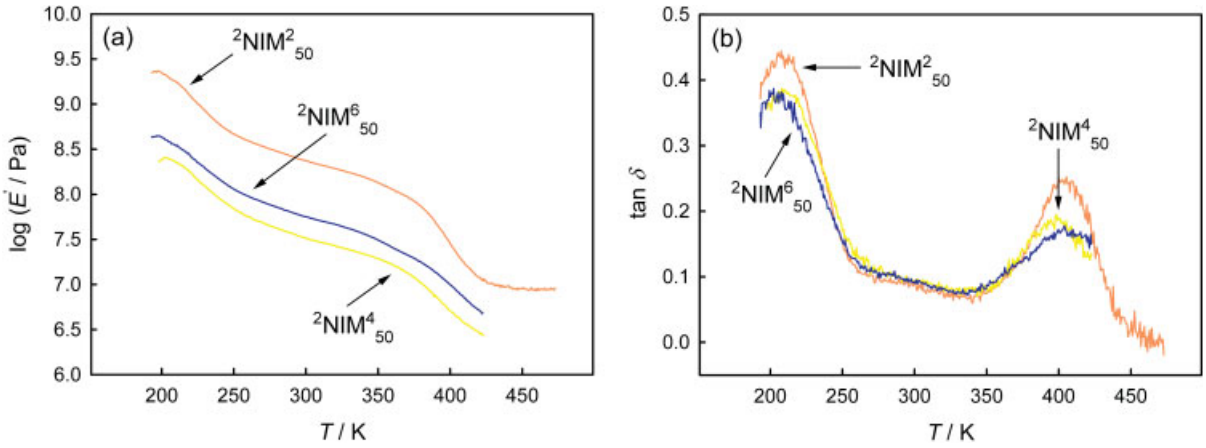


**Figure 6.** Effect of the PMMA crosslinking level on the storage modulus (a) and relaxations (b) in $^{2}NIM^{2}_{50}$ ( – ), $^{2}NIM^{4}_{50}$ ( – ) and $^{2}NIM^{6}_{50}$ ( – ).

broad distribution of correlational times with no evidence of a sharp transition between slow and fast motions. This can be explained by the motions of side chain groups distributed over a large frequency scale.

The dynamic heterogeneity observed in IPNs arises from two motionally different regions characterized by two $T_g$ values. The slow motion component is predominantly related to spin probes embedded in a phase resembling the restricted molecular motion of PMMA and NR chains of the gel phase and those close to the rigid PMMA chains. The fast component is due to the spin probes located in the mobile NR phase and interphase regions. The maximum outer extrema separation ($2A_{zz}$) measured at 100 K (rigid limit) reduces with increasing temperature. The reduced value ($2A'_{zz}$) indicates a higher mobility of the spin probe in the polymer matrix. At higher temperature, the mobilities of probe molecules in each component become comparable and only fast motional spectra are obtained. The observation of two components in all IPNs indicates dynamically different molecular environments due to the local composition fluctuations. However, this should not be taken as evidence for only two discrete dynamic states. More probably, the system has a range of chain dynamics centred on the two types of motions, as detected in the ESR experiments. This explains the broadening of the two $T_g$ values of IPNs observed by DMA.

In the range 293 – 363 K, the NR network is above its $T_g$, so the network is motionally active and the probes embedded in the network contribute to the fast component in the spectra. Higher rates of rotational motion of the probe at higher temperatures are due to the generation of larger free volumes and increased mobility of the polymer segments. The PMMA network in this temperature range is below its $T_g$ and therefore only the side chain group motions are active. The ESR spectra of the IPN with 35 wt% PMMA are complex with the appearance of the fast component at 285 K (Fig. 7, curve c), while the fast component in the spectra of pure NR appears around 268 K (Fig. 7, curve a).

IPN synthesis is considered an easy way to introduce some degree of phase mixing between two incompatible polymers. The shifting of the appearance of the fast component to higher temperature is an indication of the degree of interpenetration of the rigid PMMA network chains into the highly mobile NR networks. Interpenetration of the rigid PMMA network into the NR network stiffens the highly mobile NR network and imparts restrictions on its motional behaviour, additionally supporting the intrinsic dynamic heterogeneity within the NR matrix. The NR chains located far from the PMMA chains undergo characteristic molecular motions above their $T_g$ and those close to the rigid PMMA network chains, or highly penetrated, are subjected to restricted molecular motion, resulting in the observed $T_g$ shift to higher temperature. The SEM pictures of the same composition show that PMMA domains are highly dispersed throughout the NR matrix with the size of domains being between 30 nm and 40 nm which is an indication of enhanced phase mixing.[37] Therefore,



  

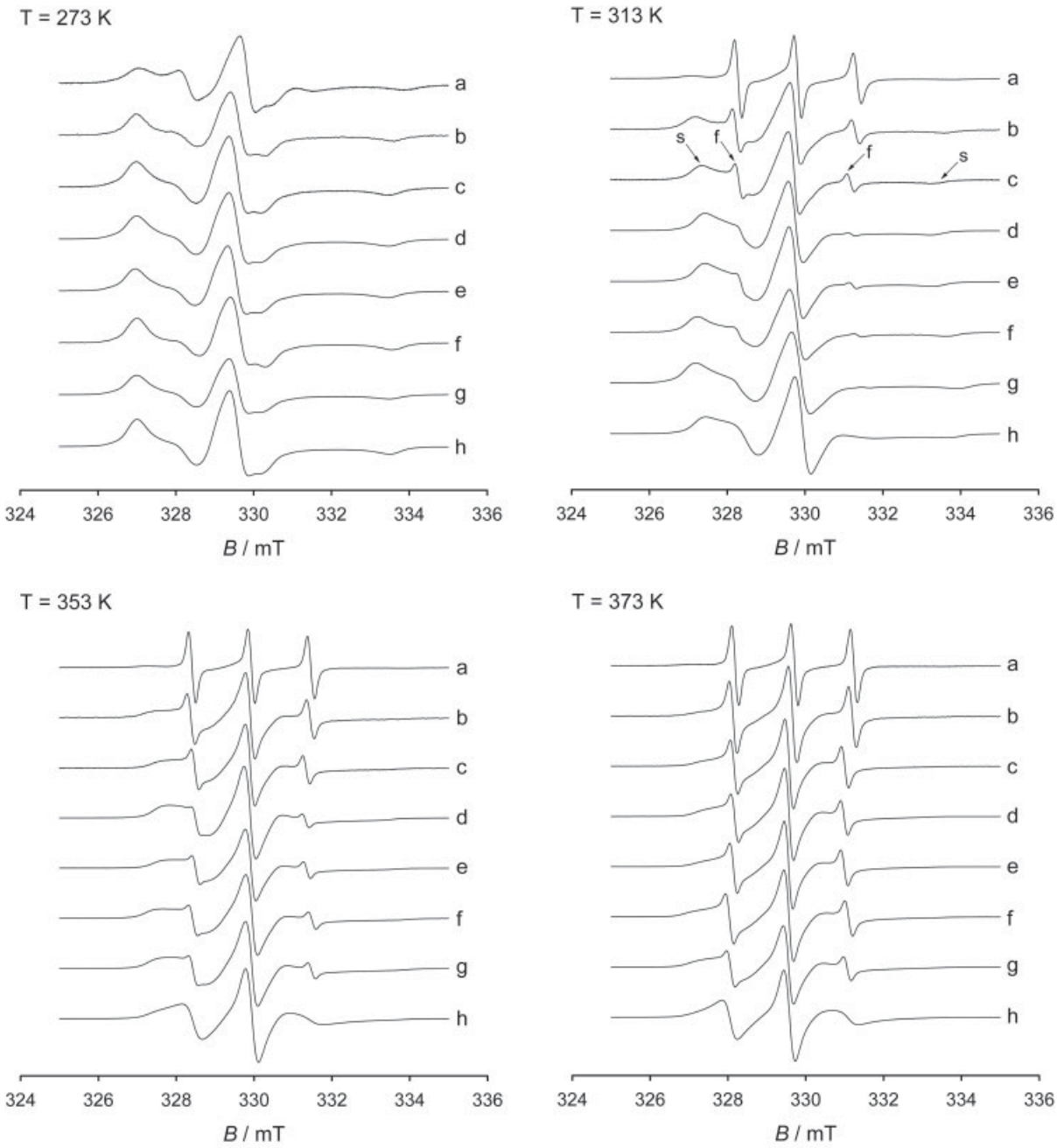


**Figure 7.** Selected ESR spectra at 273 K, 313 K, 353 K and 373 K of spin probed pure NR (curve a) and IPNs of different compositions: curve b, $^{2}NIM^{2}{}_{25}$; curve c, $^{0.8}NIM^{4}{}_{35}$; curve d, $^{2}NIM^{2}{}_{50}$; curve e, $^{4}NIM^{6}{}_{50}$; curve f, $^{4}NIM^{8}{}_{50}$; curve g, $^{0.8}NIM^{4}{}_{60}$; curve h, solitary PMMA.

high temperature is needed to overcome the motional restrictions imparted by interpenetration of the PMMA network. This shift of $T_g$ to higher temperature as a result of enhanced mixing was detected by DMA as the appearance of a shoulder on the high temperature side of the NR transition. Moreover, the DMA results show that both phases interact more effectively between each other at this particular composition. The magnitude of the shift to higher temperature is lower (17 K) compared with the semi-IPN of the same composition (25 K).[36] This is because the rubber phase is less crosslinked in the case of the full IPN (0.8 wt% of crosslinker per 100 g of NR) compared with the semi-IPN (2 wt% of crosslinker per 100 g of NR) of the same composition.[36] The crosslink density of the first formed phase (NR) has a profound influence on the degree of interpenetration between the two phases in IPNs. In full IPNs, the PMMA phase is crosslinked (4 wt% of crosslinker per 100 g of PMMA) and in semi-IPNs it is uncrosslinked.[36] Therefore the difference in the magnitude of the shift shows that interpenetration between the two phases in full IPNs is more influenced by the crosslink density of the NR phase.

Due to the characteristic molecular architecture developed during IPN synthesis, such as permanent physical entanglement of chains of both components and the penetration of the PMMA network into the entangled NR network, higher temperatures are necessary for observation of the fast component in ESR spectra. The intensity of the fast component at high temperature is smaller



  

than for pure NR. This also signifies the interaction and cooperative motional behaviour of the two components at higher temperature.

The slow component arising from the motionally restricted regions in the full IPNs mainly reflects the motional behaviour of crosslinked PMMA network chains in the highly mobile NR matrix as well as those of the NR gel phase. A part of the NR chains embedded in the gel phase show intrinsic motional restrictions in the high temperature range. NR chain segments of the gel fraction show somewhat higher values of correlational times compared with those of PMMA. In fact, this occurs at temperatures above the $T_g$ of NR where the segmental motions are active. In contrast, at this temperature the segmental motions in PMMA are still frozen and the probe dynamics are influenced only by motions of side chain groups. The close proximity and mixing of the highly mobile NR network with the PMMA network induces some flexibility in the rigid PMMA network. Therefore, the PMMA chains located in the PMMA-rich and NR-rich domains have different motional characteristics. The PMMA domains that are highly penetrated in the NR network reach their $T_g$ at a lower temperature than those located in the PMMA-rich regions. The slow component disappears around 385 K and spectra above this temperature show the characteristics of a fast moving nitroxide radical with enhanced freedom.

The low temperature spectra recorded at 193 K are similar for NR, PMMA and all the IPN samples. The fast component in the IPN with 60 wt% PMMA appears at 308 K and both slow and fast components are present up to 413 K. In 40/60 NR/PMMA IPN, the ESR spectra show the characteristics of a rigid matrix compared with pure NR and 65/35 IPN. Here the PMMA phase is more continuous than the NR phase and this can be seen in the SEM[37] and the present DMA. Therefore, the major contributions to the observed ESR spectra are arising out of the large PMMA domains. Spectra of the IPN samples $^{0.8}NIM^4_{35}$ and $^{0.8}NIM^4_{60}$ at 353 K show a very interesting phenomenon that can be realized by comparing the spectra at this particular temperature. The morphologies of these two samples are completely different. Sample $^{0.8}NIM^4_{35}$ shows a sea-island morphology with the PMMA nanodomains scattered all over the continuous NR matrix. In the case of sample $^{0.8}NIM^4_{60}$, the PMMA phase is more continuous than the NR phase.

At 353 K, the ESR spectrum of $^{0.8}NIM^4_{35}$ shows a strong slow component even though the loosely crosslinked NR phase maintains the matrix of the material. Compared with pure NR and IPN with 60 wt% PMMA, the slow component is stronger than usually expected for a sample having a highly mobile continuous matrix at high temperature. We assume that in the case of sample $^{0.8}NIM^4_{35}$ the majority of the spin probes are located in the continuous NR matrix rather than the highly dispersed PMMA domains. Therefore probes located in the NR phase have a major share in the overall contribution to the observed ESR spectra. If we assume that the contribution from the gel regions of the NR matrix is negligible at high temperature and take into account the concentration of PMMA, its dispersed morphology and the spin probe distribution in the IPN, the strong intensity of the broad component at 353 K could include a small contribution from the NR phase in addition to the major share from PMMA domains. This indicates that NR chains located close to PMMA chains are stiffened to some degree which in turn results in dynamic heterogeneity within the NR and PMMA phases. The broadening of $T_g$ values is considered an indication of phase mixing and dynamic heterogeneity. In this case, DMA showed that the $\alpha$-relaxation of NR in the IPN has a shoulder on the high temperature side of the transition due to the presence of a strong interphase (Fig. 3). We propose that this strong interphase might have contributed to the observation of a strong slow component at 353 K. Thus the ESR observation of the shift of $T_g$ to higher temperature and a strong slow component are in good agreement with the DMA observation for this particular full IPN. Sample $^{0.8}NIM^4_{60}$ shows a broad spectrum at higher temperatures, characteristic for rigid material. A small percentage of fast component can be attributed to the NR phase. Lower crosslinking in NR and a high PMMA content makes the rigid phase more dominant and continues in this sample. Both DMA and previous SEM[37] analysis showed that the PMMA phase was dominant and more continuous. Therefore we propose that the shape of the ESR spectrum can be used to arrive at some morphological conclusions with the help of other techniques like SEM, TEM and DMA given that one of the components should be elastic and the other a rigid polymer.

Selected ESR spectra of moderately crosslinked IPNs with different PMMA contents, $^{2}NIM^2_{25}$ and $^{2}NIM^2_{50}$, are shown in Fig. 7, curves b and d. The spectra of these samples at low temperatures are similar to those of pure NR. The influence of 25 wt% PMMA (sample $^{2}NIM^2_{25}$) can be seen above 273 K, where the spectra are completely different from those of pure NR, measured at the same temperature. The fast component appears at 280 K and this indicates that the presence of PMMA induces motional restriction in the NR phase. The IPN shows a sea-island morphology in SEM analysis[37] and only one transition corresponding to NR is observed in the DMA tan $\delta$ scan. Our previous studies on semi-IPNs reveal that the interaction between the NR and PMMA phases is maximal around 35 wt% of PMMA content. The slow component in spectra of the $^{2}NIM^2_{25}$ sample originates from the spin probes embedded in the PMMA domains and the NR network in the immediate vicinity of the PMMA domains. IPN formation with the NR makes the rigid PMMA more flexible and, as a result, the slow component disappears at 380 K.

The $^{2}NIM^2_{50}$ sample has a broad spectrum compared with that of $^{2}NIM^2_{25}$ (the slow component is present up to 413 K). SEM and TEM analysis[37] show that the $^{2}NIM^2_{50}$ IPN possesses a nanostructure morphology which contributes to the sample rigidity. In this case the fast component appears at 300 K which clearly indicates that the crosslinked PMMA network stiffens the NR network at the molecular level, thereby introducing motional restrictions in the NR chains. The DMA of this IPN shows an inward shift in $T_g$ values of both components which indicates a better interpenetration between the two phases and supports the above observation.

ESR spectra of IPNs with different crosslink densities in the NR and PMMA phases are compared at 353 K. It can be seen that the highly crosslinked IPNs ($^{4}NIM^6_{50}$ and $^{4}NIM^8_{50}$) have more mobile component than $^{2}NIM^2_{50}$. This supports the fact that higher crosslinking in the first formed phase enhances the interpenetration between the two phases. This induces some degree of flexibility in highly rigid PMMA network chains and restricts the chain motion of highly mobile NR chains in the interphase developed around the PMMA nanodomains. Also, higher crosslinking in the NR phase decreases the PMMA domain size, indicating phase mixing, and leads to a more continuous NR phase in the IPNs. The above observation is confirmed by DMA in which the $T_g$ values of both phases show an inward shift. Different crosslink densities in the PMMA phase (6 wt% and 8 wt%) seems to have no significant influence on the ESR spectra.

The best method to calculate rotational correlation times ($\tau_c$) is a spectral simulation. An alternative method that allows a reasonable estimation of $\tau_c$ in the slow motional regime can be



  

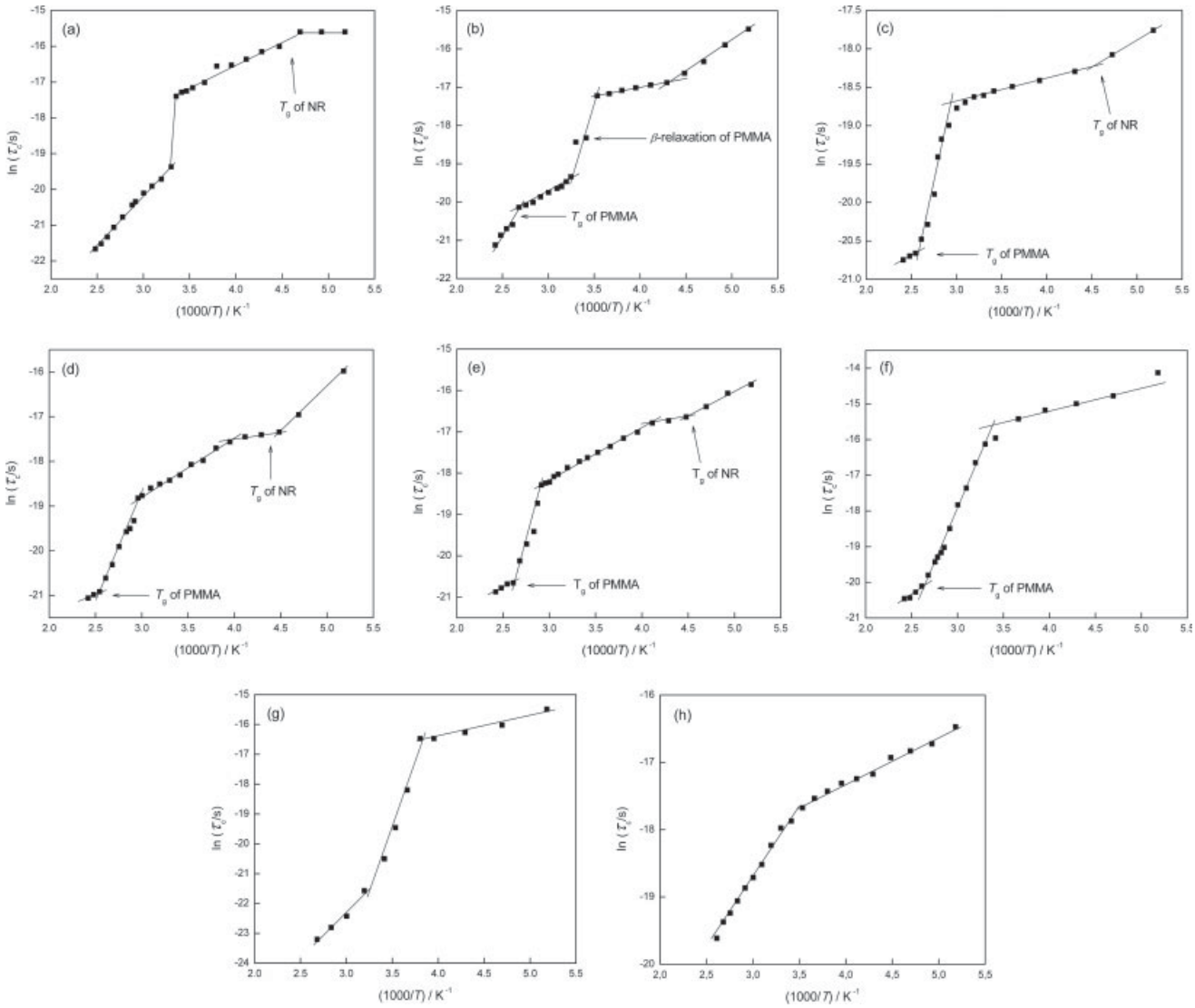


**Figure 8.** Arrhenius plots of ln $\tau_c$ *versus* 1/*T*: (a) $^{2}NIM^{2}_{25}$; (b) $^{0.8}NIM^{4}_{35}$; (c) $^{2}NIM^{2}_{50}$; (d) $^{4}NIM^{6}_{50}$; (e) $^{4}NIM^{8}_{50}$; (f) $^{0.8}NIM^{4}_{60}$; (g) pure NR; (h) solitary PMMA.

obtained from the temperature dependence of $2A'_{zz}$[32]:

$$\tau_c = a\,(1-S)^b \qquad (1)$$

where $S = 2A'_{zz}/2A_{zz}$. The Brownian diffusion model was used for the present study and an intrinsic linewidth of 8 G was calculated from a simulation of rigid limit spectra for a semi-IPN at 100 K. For these conditions, the values of *a* and *b* are $1.10 \times 10^{-9}$ and −1.01, respectively. The correlation times in the high temperature regime can be calculated from[32]

$$\tau_c = 0.65 \times 10^{-9}\Delta B\left(\left[\frac{I(0)}{I(-1)}\right]^{1/2} + \left[\frac{I(0)}{I(+1)}\right]^{1/2} - 2\right) \qquad (2)$$

where $I(-1)$, $I(0)$ and $I(+1)$ are the intensities of low, central and high field lines, respectively, and $\Delta B$ is the linewidth of the central line. The $\tau_c$ calculations were performed for both fast and slow motional regions. For the slow motional region $\tau_c$ was estimated from Eqn (1) up to a temperature where *S* was undefinable, since the outer lines began to converge to the motionally narrowed spectrum and $\tau_c$ values of the slow and fast components became almost indistinguishable. Equation (2) for the fast motional region was used to calculate $\tau_c$ from the temperature at which the ESR spectrum showed relatively sharp hyperfine lines up to 413 K.

Arrhenius plots of ln $\tau_c$ *versus* 1000/*T* for the IPNs are shown in Fig. 8. Several motional regions can be seen for IPNs in the temperature range 183–413 K. Four crossover points for samples $^{0.8}NIM^{4}_{35}$, $^{4}NIM^{6}_{50}$ and $^{4}NIM^{8}_{50}$, three for samples $^{2}NIM^{2}_{25}$ and $^{2}NIM^{2}_{50}$, two for $^{0.8}NIM^{4}_{60}$ and pure NR and one for solitary PMMA can be observed. The existence of several crossover points can be explained as follows. The low temperature (183–233 K) and high temperature (348–393 K) crossover points coincide with the glass transitions of NR and PMMA, respectively (sample $^{0.8}NIM^{4}_{60}$ does not show the distinct motional region associated with the $T_g$ of the NR phase). We found that the nature of probe motion is heavily influenced by the molecular motions associated with the PMMA segments. The activation energies determined in the $T_g$ region of NR for all IPN samples are found to be the same within the experimental uncertainty, i.e. $E_a$ (low temperature) = 13.0 ± 3.0 kJ mol$^{-1}$. This suggests that regardless of the model used in the calculation of correlation times, the molecular motions of the probe are activated by the same



  

molecular process. Although the activation energies are much lower compared with the values usually observed in the $T_g$ region, it can be suggested that the observed dynamics are correlated to the $\alpha$-relaxation of NR. This motional region, as shown in Fig. 8, follows the same trends of shifts in position of the $\alpha$-relaxation in NR as observed by DMA. Two crossover points for pure NR detected at 268 K and 313 K are associated with the beginning of segmental motions in the sol and gel phase, respectively. The shift of these temperature points in IPNs is affected by both the $\beta$-relaxation in PMMA and the degree of chain interpenetration. The influence of $\beta$-relaxation seems to play a major role at lower temperature, while the degree of interpenetration dominates at higher temperature. Consequently, two to four crossover points are detected in IPNs, depending on the composition and crosslinking degrees. In the case of solitary PMMA, only one weakly expressed crossover point is detected around 283 K. This should be attributed to changes in the motion of side groups.

An interesting phenomenon is observed in the case of $^{0.8}NIM^4_{35}$ (Fig. 8(b)), which has four crossover points. The $\beta$-relaxation corresponding to PMMA is detected from the plot of ln $\tau_c$ *versus* 1000/$T$ in the region 283–313 K. Among all the semi-IPNs and full IPNs studied, only this particular full IPN shows a strong $\beta$-relaxation in this region, also in DMA. The activation energy ($E_a$) estimated from the Arrhenius plot of ln $\tau_c$ *versus* 1000/$T$ for this temperature region is found to be 53.4 kJ mol$^{-1}$. This value is in good agreement with the standard value reported for PMMA (65.0 kJ mol$^{-1}$ obtained through DMA by Perkin Elmer). The slightly lower value in our case explains the shift of the $\beta$-relaxation peak to lower temperature compared with solitary PMMA in DMA.

Activation energies in the region 243–313 K for all other IPNs are found to be $7.0 \pm 2.0$ kJ mol$^{-1}$. These values are in agreement with those reported for similar systems.[28] At temperatures below the $T_g$ of PMMA, the probe is activated by local relaxation modes in the polymer matrix which are generally characterized by small activation energies. In the high temperature region $E_a$ values are 23.2 kJ mol$^{-1}$, 44.7 kJ mol$^{-1}$, 24.9 kJ mol$^{-1}$, 50.5 kJ mol$^{-1}$, 35.5 kJ mol$^{-1}$ and 54.6 kJ mol$^{-1}$ for $^{0.8}NIM^4_{35}$, $^{0.8}NIM^4_{60}$, $^{2}NIM^2_{25}$, $^{2}NIM^2_{50}$, $^{4}NIM^6_{50}$ and $^{4}NIM^8_{50}$ samples, respectively. The higher values compared with the low temperature region are in good agreement with previous studies.[28,29] Among the IPNs studied, those having lower PMMA content ($^{2}NIM^2_{25}$ and $^{0.8}NIM^4_{35}$, Figs. 8(a), 8(b)) show the lowest $E_a$ values in the high temperature region. This is because of the flexibility induced in the PMMA chains as a result of phase mixing with the highly mobile NR chains during IPN formation. Since $E_a$ shows a trend that can be correlated to the level of mixing between the NR and PMMA networks, it can be suggested that the probes reflect motional characteristics of the interphase regions. Low activation energy is required for those PMMA chains that are in close proximity (or mixed) with the highly mobile NR chains. Even though the activation energies are much lower than the values usually observed in the $T_g$ region (200–400 kJ mol$^{-1}$), we suggest that the motion of the probe in this region is correlated with the $\alpha$-relaxation of PMMA because it was found that $T_{5mT} \approx T_g$ for the rigid component ($T_{5mT}$ is defined as the temperature at which external extrema separation reaches 5 mT).[32] Consequently, the probe should be located in the PMMA segment whose motion is activated at $T_g$.

The $T_{5mT}$ corresponding to the broad component is related to $T_g$ of PMMA in the full IPNs, as previously observed in semi-IPNs.[36] Considering the broad range of $T_g$ values observed in full IPNs by DMA and the different methodology used in ESR, the $T_{5mT}$ values obtained fall within the range of error of less than 8 K. For example, for the IPN with 40/60 composition ($^{0.8}NIM^4_{60}$), the $T_{5mT}$ of the rigid component falls exactly in the region of the main relaxation of PMMA ($T_{5mT} = T_g = 402$ K). Other full IPNs also show the same trend as above. In the case of highly crosslinked IPN with 50:50 composition ($^{4}NIM^6_{50}$), the $T_{5mT}$ value is shifted to lower temperature (385 K) which is in good agreement with the inward shifting of $T_g$ observed in DMA.

### $^{13}C$ $T_{1\rho}$ relaxation of IPNs

The $^{13}C$ $T_{1\rho}$ relaxation times, unlike the corresponding $^{1}H$ $T_{1\rho}$ relaxation times, are not influenced by spin diffusion, and therefore the relaxation of each carbon can be detected. In the $^{13}C$ $T_{1\rho}$ pulse sequence carbon magnetization is built up via cross-polarization, and the carbons are held in the rotating frame without direct contact with the proton reservoir for a variable period $\tau$, allowing the $^{13}C$ polarization to decay in its own rotating field. This structure of the pulse sequence results in sensitivity of $^{13}C$ $T_{1\rho}$ to molecular motion in the frequency range 10–100 kHz, characteristic for relatively long-range cooperative motions of polymer chains below the glass transition. The $^{13}C$ $T_{1\rho}$ relaxation is the sum of spin–lattice and spin – spin relaxation processes. The spin – spin process generally becomes significant in determining the $^{13}C$ $T_{1\rho}$ of highly crystalline polymers.[34] Schaefer *et al.* have concluded that in glassy polymers the spin–lattice component is dominant and that the $^{13}C$ $T_{1\rho}$ is predominantly determined by motional processes for spin-locking frequencies greater than 30 kHz.[33,34,40] There are a large number of papers showing that $^{13}C$ $T_{1\rho}$ is dominated by spin–lattice processes in amorphous polymers in both the glassy and rubbery states.[33,34,40,41] Therefore the $^{13}C$ $T_{1\rho}$ relaxation times can be effectively utilized to investigate the motion of PMMA chains in the homopolymer and in IPNs below $T_g$. The carbon resonance intensity decays with a time constant equal to the $^{13}C$ $T_{1\rho}$ by an exponential function:

$$M(\tau) = M(0) \quad \exp\left(-\tau/T_{1\rho}\right) \tag{3}$$

Thus the slope of a logarithmic plot of the magnetization intensity $M(\tau)$ *versus* delay time $\tau$ yields the $^{13}C$ $T_{1\rho}$ value.

The signal from the NR phase could not be followed because of very low intensity. This is due to low dipolar coupling in the highly mobile NR phase and thus cross-polarization will not be effective. The $^{13}C$ $T_{1\rho}$ relaxations of full IPNs are shown in Table 1. As in semi-IPNs, PMMA carbon atoms in full IPNs also showed two relaxations, fast and slow, except for the quaternary carbon atom. The presence of two relaxation times indicated the close proximity

**Table 1.** $^{13}C$ $T_{1\rho}$ relaxations of PMMA and selected IPN samples

| Sample | >C=O 182 ppm | | –CH$_2$– and –OCH$_3$ 56 ppm | | >C< 49 ppm | | $\alpha$-CH$_3$ 21 ppm | |
|---|---|---|---|---|---|---|---|---|
| | Short ms | Long ms | Short ms | Long ms | Short ms | Long ms | Short ms | Long ms |
| PMMA | 4.14 | | 2.16 | | 1.49 | | 2.15 | |
| $^{0.8}NIM^4_{35}$ | 4.12 | 53.27 | 4.75 | 16.22 | 6.60 | | 4.54 | 17.24 |
| $^{0.8}NIM^4_{60}$ | 4.17 | 42.07 | 3.18 | 20.13 | 6.09 | | 3.23 | 14.31 |
| $^{2}NIM^6_{50}$ | 4.57 | 43.44 | 0.61 | 8.09 | 2.50 | 9.49 | 2.61 | 48.85 |
| $^{2}NIM^2_{50}$ | 11.33 | 29.86 | 7.17 | 161.2 | 5.58 | | 2.50 | 11.10 |



  

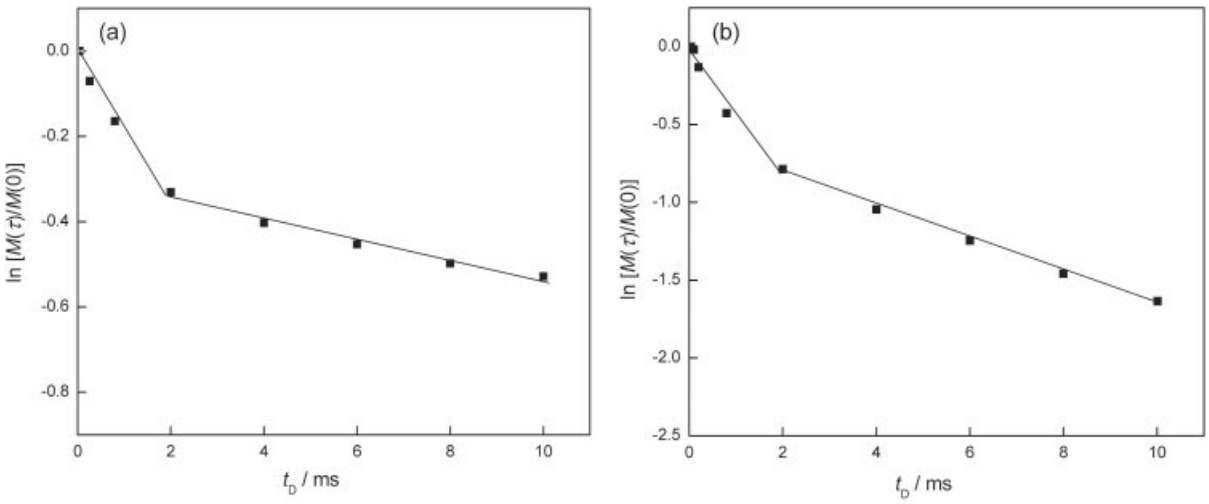


**Figure 9.** Relaxations of carbonyl carbon in IPN sample $^{0.8}NIM^{4}_{35}$ (a) and quaternary carbon in highly crosslinked IPN ($^{2}NIM^{6}_{50}$) (b).

of two types of molecular environment. So the short and long relaxation components can be attributed to those arising from PMMA-rich and NR-rich regions. The carbonyl carbon in the IPN sample $^{0.8}NIM^{4}_{35}$ has the slowest relaxation of all the IPNs studied. The DMA and ESR studies demonstrated that of all the IPNs studied this particular IPN shows maximum interaction between the two phases. We suggest that the long relaxation is due to the strong interaction between PMMA and NR chains. Figure 9(a) shows the relaxations of carbonyl carbon in the $^{0.8}NIM^{4}_{35}$ sample. The $\beta$-relaxation observed in this particular IPN is due to the rotation of the –COOH group. This relaxation was found to be shifted to lower temperature for the same IPN which indicated that the –COOH group is rotating with enhanced freedom. The slow relaxation in the carbonyl carbon suggests that some of the carbonyl groups are intimately mixed with the highly mobile NR chains and as a result the carbonyl groups have a higher degree of motional freedom. Very interestingly, the relaxation time of the quaternary carbon atom shows a slight increase for samples $^{0.8}NIM^{4}_{60}$, $^{0.8}NIM^{4}_{35}$ and $^{2}NIM^{2}_{50}$. The higher mobility of the attached carbon atoms due to mixing with NR chains might have led to a slightly longer relaxation for the quaternary carbon atom. The relaxation in highly crosslinked IPN ($^{2}NIM^{6}_{50}$) seems to be much faster due to the increased rigidity of the matrix. At the same time, higher crosslinking increases the degree of interpenetration between the two phases. This may have resulted in two relaxations, short and long, for the quaternary carbon atom in highly crosslinked IPN ($^{2}NIM^{6}_{50}$). Figure 9(b) shows the decay of carbon magnetization in quaternary carbon atoms. The long component of relaxation reveals the degree of flexibility imparted on PMMA chains due to the close proximity of highly mobile NR chains. This high level of interpenetration may have also resulted in a very long component of decay in rotating methyl groups (21 ppm).

## CONCLUSIONS

Dynamic mechanical spectra of NR/PMMA sequential full IPNs are presented. The immiscible polymers show a reasonable degree of compatibility during IPN formation especially when the PMMA concentration is less than 40 wt%. Crosslinking of the second phase showed increased miscibility; therefore full IPNs show a higher degree of interpenetration than semi-IPNs. Also, a lower concentration of PMMA is found to shift the $\alpha$-relaxation of NR to higher temperature and induces motional heterogeneity in the NR networks. IPNs show an increase in the storage modulus with increasing PMMA content up to 473 K, despite a decrease after the PMMA transition. Highly phase separated IPNs show a complete drop of modulus at 423 K. NR/PMMA 65/35 IPN shows a broad transition arising from $\beta$- and $\alpha$-relaxations of PMMA with the $\beta$-relaxation slightly shifting towards lower temperature due to a higher degree of motional freedom attained by the PMMA network upon mixing with the highly mobile NR phase. Higher crosslinking in the NR phase is shown to increase miscibility and shifts transitions closer to each other. A heavily crosslinked NR network also leads to broadening of transitions due to overlapping of several relaxation processes. A high degree of crosslinking in PMMA increases phase separation and is found to have no effect on the $\beta$-relaxations of the PMMA chains, but medium level crosslinks are needed for better interpenetration between phases. The ESR results show that PMMA chains located in the PMMA-rich and NR-rich domains have different motional characteristics. Moreover the influence of rigid PMMA chains on the motional behaviour of NR chains was also observed. The strong interaction between PMMA and NR chains was also detected by carbonyl relaxation in solid state NMR spectra.

## ACKNOWLEDGEMENTS

The authors acknowledge R. Suriyakala, PSE UMASS, Amherst, USA, for her technical support during the research work. This study was supported by the Department of Science and Technology (DST) (Project no. INT/CROATIA/P-8/05), Government of India, and the Ministry of Science, Education and Sports of the Republic of Croatia (Projects 062-0000000-3209 and 098-0982915-2939).

## REFERENCES

1 Lipatov YS and Alekseeva TT, *Adv Polym Sci* **208**:1–227 (2007).
2 Sperling LH, *Interpenetrating Polymer Networks and Related Materials*. Plenum Press, New York (1981).
3 Huelck V, Thomas DA and Sperling LH, *Macromolecules* **5**:340–348 (1972).
4 Donatelli AA, Sperling LH and Thomas DA, *Macromolecules* **9**:671–675 (1976).
5 Widmaier JM and Sperling LH, *Macromolecules* **15**:625–631 (1982).
6 Donatelli AA, Sperling LH and Thomas DA, *J Appl Polym Sci* **21**:1189–1197 (1977).

  

7 Thomas DA and Sperling LH, Interpenetrating polymer networks, in *Polymer Blends*, ed. by Paul DR and Newman S. Academic Press, San Diego (1978).
8 Bauer BJ and Briber RM, The effect of crosslink density on phase separation in interpenetrating polymer networks, in *Advances in interpenetrating polymer networks*, ed. by Klempner D and Frisch KC. Technomic Publishing, Lancaster (1994).
9 Alves NM, Ribelles JLG, Tejedor JAG and Mano JF, *Macromolecules* **37**:3735–3744 (2004).
10 Mathew AP, *Interpenetrating Polymer Networks Based on Natural Rubber and Polystyrene*. Mahatma Gandhi University, Kottayam, Kerala, India (2001).
11 Wang M, Pramoda KP and Goh SH, *Chem Mater* **16**:3452–3456 (2004).
12 Rohman G, Grande D, Laupretre F, Boileau S and Guerin P, *Macromolecules* **38**:7274–7285 (2005).
13 Pionteck J, Hu JJ and Schulze U, *J Appl Polym Sci* **89**:1976–1982 (2003).
14 Mathew AP, Packirisamy S and Thomas S, *J Appl Polym Sci* **78**:2327–2344 (2000).
15 Mathew AP, Packirisamy S, Radusch HJ and Thomas S, *Eur Polym J* **37**:1921–1934 (2001).
16 Ngai KL and Rendell RW, *J Non-Cryst Solids* **131**:942–948 (1991).
17 Kramarenko VY, Ezquerra TA, Sics I, Balta-Calleja FJ and Privalko VP, *J Chem Phys* **113**:447–452 (2000).
18 Roland CM, *Macromolecules* **27**:4242–4247 (1994).
19 Prochazka F, Durand D and Nicolai T, *J Rheol* **43**:1511–1524 (1999).
20 Berzosa AE, Ribelles JLG, Kripotou S and Pissis P, *Macromolecules* **37**:6472–6479 (2004).
21 Kyritsis A, Ribelles JLG, Duenas JMM, Campillo NS, Ferrer GG and Pradas MM, *Macromolecules* **37**:446–452 (2004).
22 Landry CJT and Henrichs PM, *Macromolecules* **22**:2157–2166 (1989).
23 Rizos AK, Fytas G, Ma RJ, Wang CH, Abetz V and Meyer GC, *Macromolecules* **26**:1869–1875 (1993).
24 Miwa Y, Drews AR and Schlick S, *Macromolecules* **41**:4701–4708 (2008).
25 Miwa Y, Sugino Y, Yamamoto K, Tanabe T, Sakaguchi M, Sakai M *et al.*, *Macromolecules* **37**:6061–6068 (2004).
26 Wolinska-Grabczyk A, Bednarski W, Jankowski A and Waplak S, *Polymer* **46**:2461–2471 (2005).
27 Wasserman AM, Yasina LL, Motyakin MV, Aliev, II, Churochkina NA, Rogovina LZ *et al.*, *Spectrochimica Acta Mol Spectroscopy* **69**:1344–1353 (2008).
28 Müller G, Stadler R and Schlick S, *Macromolecules* **27**:1555–1561 (1994).
29 Schlick S, Harvey RD, Alonso-Amigo MG and Klempner D, *Macromolecules* **22**:822–830 (1989).
30 Qiu FR, Chen SM and Ping ZH, *Magn Reson Chem* **43**:411–416 (2005).
31 Valić S, Rakvin B, Veksli Z and Grubišić-Gallot Z, *Macromolecules* **23**:5182–5186 (1990).
32 Veksli Z, Andreis M and Rakvin B, *Prog Polym Sci* **25**:949–986 (2000).
33 Schaefer J, Stejskal EO and Buchdahl R, *Macromolecules* **10**:384–405 (1977).
34 Jack KS and Whittaker AK, *Macromolecules* **30**:3560–3568 (1997).
35 Wu RR, Kao HM, Chiang JC and Woo EM, *Polymer* **43**:171–176 (2002).
36 John J, Klepac D, Didović M, Sandesh CJ, Liu Y, Raju KVSN *et al.*, *Polymer* **51**:2390–2402 (2010).
37 John J, Suriyakala R, Thomas S, Mendez JM, Pius A and Thomas S, *J Mater Sci* **45**:2892–2901 (2010).
38 Sanchez MS, Ferrer GG, Cabanilles CT, Duenas JMM, Pradas MM and Ribelles JLG, *Polymer* **42**:10071–10075 (2001).
39 Marinović T, Valić S, Andreis M and Veksli Z, *Polymer* **32**:2519–2522 (1991).
40 Schaefer J, Stejskal EO, Steger TR, Sefcik MD and Mckay RA, *Macromolecules* **13**:1121–1126 (1980).
41 Schaefer J, Sefcik MD, Stejskal EO and Mckay RA, *Macromolecules* **17**:1118–1124 (1984).




  